Article

Impacts of the Surface Potential Vorticity Circulation over the Tibetan Plateau on the East Asian Monsoon in July

Yimin Liu [1,2], Lulu Luan [1], Guoxiong Wu [1,2,*] and Tingting Ma [1,*]

[1] State Key Laboratory of Numerical Modelling for Atmospheric Sciences and Geophysical Fluid Dynamics (LASG), Institute of Atmospheric Physics (IAP), Chinese Academy of Sciences (CAS), Beijing 100029, China; lym@lasg.iap.ac.cn (Y.L.); luanlulu@lasg.iap.ac.cn (L.L.)

[2] College of Earth and Planetary Sciences, University of Chinese Academy of Sciences, Beijing 100049, China

* Correspondence: gxwu@lasg.iap.ac.cn (G.W.); matingting@lasg.iap.ac.cn (T.M.)

Abstract: Based on the definition of potential vorticity substance (W) and its equation, an index "iPV" representing the leading mode of the surface potential vorticity circulation (PVC) over the Tibetan Plateau is defined to characterize the orographic potential vorticity (PV) forcing on the atmospheric general circulation. The relationships between the iPV index and the East Asian monsoon in July, as well as the Silk Road pattern in Eurasia, are investigated on an interannual time scale. Results show that the iPV in July is closely related to the interannual variability of the East Asian monsoon. Corresponding to the positive phase of iPV with negative (positive) PVC over the north (south) of the plateau, strong positive PV anomalies and westerly flows develop in the troposphere over the plateau. Consequently, in the downstream region, the zonal PV advection increases with height just above the Jianghuai Meiyu front, which is conducive to the generation of upward movement. Over the East Asian area, the upper troposphere is controlled by the eastward shifted South Asian High. In the lower troposphere, the southwesterly flow anomaly on the northwestern side of the strengthened western Pacific subtropical high transports abundant water vapor to the north, forming a convergence in the Jianghuai area, leading to the formation of large-scale precipitation along the Meiyu front. Results from partial correlation analysis also demonstrate that the link between the variability of the East Asian monsoon in July and the plateau PV forcing is affected very little by the Silk Road pattern, whereas the plateau PV forcing plays a key "bridging" role in the influence of the Silk Road pattern on the East Asian monsoon.

Keywords: potential vorticity substance; potential vorticity circulation; East Asian monsoon; Tibetan Plateau

1. Introduction

The East Asian summer monsoon (EASM) is a complex monsoon system composed of multiple important components such as tropospheric upper circulations, lower circulations, and precipitation. The seasonal evolution of the EASM is accompanied by the advance of the rain belt from south to north and has significant differences in interannual variation during different periods [1]. According to the definition of East Asian monsoon intensity [2], there exist significant differences in the intensity and pattern of EASM in different months of summer. Other studies even show that some factors that influence the interannual variability of the EASM also exhibit intra-seasonal differences [3,4].

Previous studies have shown that the Tibetan Plateau has significant impacts on the EASM through dynamical and thermodynamical effects. The dynamical forcing of the plateau has a very important impact on the establishment, development, evolution, and precipitation of the monsoon. The thermodynamic forcing mainly comes from the heating of the plateau, which is the main driver of EASM precipitation [5]. Numerous studies have been contributed to investigate the separate influence of either the dynamical forcing of the Tibetan Plateau [6,7] or its thermal forcing [8–10] on the EASM. For example, Okajima

and Xie [7] find that the uplifted terrain plays an important role in the formation of the northwestern Pacific monsoon, while Duan and Wu [10] emphasize the role of the thermal forcing of the Tibetan Plateau in influencing the summer climate patterns over subtropical Asia. The study of the influence on the EASM of the combined mechanical and thermal forcing of the Tibetan Plateau is rare.

As we all know, PV is defined as $P = \frac{1}{\rho}\vec{\zeta}_a \cdot \nabla\theta$, where ρ is air density, $\vec{\zeta}_a$ is three-dimensional absolute vorticity, and θ is potential temperature. It is a physical quantity that combines the intrinsic dynamic and thermodynamic characteristics of the atmosphere. The huge uplift Tibetan Plateau has been proven the most important PV source in the world. The surface PV over the Tibetan Plateau may better represent the plateau forcing and have a closer relationship with the EASM. Sheng et al. [11,12] and He et al. [13] have demonstrated that the surface PV over the Tibetan Plateau can have a significant impact on the interannual variation of summer precipitation in East Asia via changing the atmospheric circulations. In this study, we study the PV circulation (PVC) at the surface of the Tibetan Plateau, rather than the PV within the surface layer, and reveal the relationship between the surface PVC of the plateau and the EASM.

Interestingly, the circulation structure and precipitation anomalies over the EASM region in July induced by the above-mentioned PVC forcing over the Tibetan Plateau look similar to those associated with the "Silk Road" pattern (SRP) in summer over the troposphere of Eurasia, which has been considered the main mode of the meridional wind anomaly [14]. The quasi-stationary Rossby remote-correlated wave train over the Asian troposphere in July in the Northern Hemisphere can affect the climate of a vast area along the axis of the Asian subtropical jet stream (about 40° N) [15–17] and has a significant impact on the circulation and precipitation of the tripolar type of the EASM [4,18,19]. The Tibetan Plateau is located along the Rossby wave train induced by the SRP and upstream of the EASM region. It is still unclear whether the Tibetan Plateau can modulate the effect of the SRP on EASM or not. What role the Tibetan Plateau plays in the relationship between the SRP and EASM needs clarification.

This paper aims to explore the influence on the EASM of the surface PVC forcing over the Tibetan Plateau in July, and the relationship between the circulation anomalies induced by the PVC forcing over the Tibetan Plateau and by the SRP. The context of the study is arranged as follows: Section 2 introduces the data used for the study and the concept of surface potential vorticity circulation (SPV). Section 3 demonstrates the July-mean global distributions of SPV and its zonal deviation, and an index presenting the SPV forcing of the Tibetan Plateau, i.e., iPV, is thereby introduced. By using this iPV index, the impact of the SPV forcing of the Tibetan Plateau on the EASM is studied by using regression analysis in Section 4. In Section 5, the influence on the EASM of the SPV forcing of the Tibetan Plateau is compared with the impact on the EASM of the SRP forcing by using partial correlation analysis. Conclusions are provided in Section 6.

2. Data and Methods

2.1. Data

The data of atmospheric variables used to calculate the surface PVC over the Tibetan Plateau were obtained from the daily reanalysis data at the bottom (level = 72, σ = 0.993) of the MERRA-2 (Modern-Era Retrospective Analysis for Research and Applications Version 2) published by NASA [20]. The variables include the horizontal wind, temperature, and pressure with a horizontal resolution of 0.625 × 0.5° (longitude × latitude). The atmospheric data used in the diagnostic analysis of the atmospheric circulation are from monthly data under the MERRA2 barometric coordinate system, including Ertel potential vorticity (EPV), horizontal wind, geopotential height, specific humidity, and surface pressure with a horizontal resolution of 0.625 × 0.5° (longitude × latitude). Precipitation data are monthly averaged data provided by the Global Precipitation Climatology Project, version 2.3 [21] with a horizontal resolution of 2.5 × 2.5° (longitude × latitude). The time span is from 1980 to 2019 for all datasets.

To focus on the relationship between interannual variations, all variable data were preempted with detrending and 2–9 year Lanczos bandpass filtering to preserve interannual signals.

2.2. Partial Correlation Analysis

Partial correlation refers to the method of studying the correlation between only two variables while another variable remains unchanged in a multivariate study [22]. In actual research work, it is common to find that one of the three variables remains unchanged and the correlation between the other two variables is explored. When the influence of the sequence Z(t) is excluded, the partial correlation coefficient between the sequence X(t) and Y(t) is calculated as follows:

$$r_{xy,z} = \frac{r_{xy} - r_{xz}r_{yz}}{\sqrt{(1 - r_{xz}^2)(1 - r_{yz}^2)}}$$

where r_{xy}, r_{xz}, and r_{yz} are, respectively, the correlation coefficients between sequence X(t) and Y(t), X(t) and Z(t), and Y(t) and Z(t); and $r_{xy,z}$ is the partial correlation coefficient, which represents the correlation coefficient between sequence X(t) and sequence Y(t) after excluding the influence of time series Z(t). Student's t-test is used to determine the confidence level of the partial correlation coefficient, and the test statistic quantity t with a sample size *n* is:

$$t = \frac{r\sqrt{n - 3}}{\sqrt{1 - r^2}}$$

2.3. Earth's Surface PVC Forcing-SPV

PV substance (W) is defined as Refs. [23,24]:

$$W = \rho P = \nabla \cdot (\vec{\zeta}_a \theta) \tag{1}$$

The local variation equation for PV substance (also known as potential vorticity density) can be rewritten in flux form:

$$\frac{\partial W}{\partial t} = -\nabla \cdot \left[W\vec{V} - (Q\vec{\zeta}_a + \theta\vec{F}) \right] = -\nabla \cdot \vec{J} \tag{2}$$

From Equations (1) and (2),

$$\nabla \cdot \frac{\partial}{\partial t}(\vec{\zeta}_a \theta) = -\nabla \cdot \vec{J} \tag{3}$$

Equation (2) shows that the local variation of PV substance is related to its advection, diabatic heating, and friction. In Equation (3), $\vec{J}$ represents the "effective potential vorticity flux" that affects the local change of W.

By defining the PV circulation (PVC) as [25]:

$$\vec{J_C} = -\vec{\zeta}_a \theta = \int_{t_0}^{t_0 + \triangle t} \vec{J} \, dt + \vec{C} \tag{4}$$

Then we have:

$$W = -\nabla \cdot (\vec{J_C}) \tag{5}$$

In the pressure coordinate system with unit vectors ($\vec{i}$, $\vec{j}$, $\vec{k}$) pointing eastward, northward, and downward, respectively,

$$\vec{J_C} = (J_C^x, J_C^y, J_C^p) = -\frac{\partial v}{\partial p}\theta\,\vec{i} + \frac{\partial u}{\partial p}\theta\,\vec{j} + (f + \frac{\partial v}{\partial x} - \frac{\partial u}{\partial y})\theta\,\vec{k} \tag{6}$$

In Equation (4), the physical interpretation of PVC is the time accumulated effective potential vorticity flux. Equation (5) indicates that the convergence (divergence) of PVC corresponds to a positive (negative) PV substance (W). When we consider the total PV substance of a global atmosphere covered by an upper boundary "top" of an isentropic surface θ_T (e.g., 390 K), we need to perform a global integration for W. By employing the Gaussian theorem to convert the global volume integration of W into a surface integration of the crossing boundary PVC over the boundary surfaces (S) enclosing the global volume, we can obtain:

$$\underbrace{\iiint_{\text{Globe}} W dv} = \iiint_{Globe} -\nabla \cdot (\vec{J_C}) dx dy dp = \oiint_{S} -(\vec{J_C} \cdot \vec{n}) ds = \underbrace{\iint_{top} J_C^p dx dy} + \underbrace{\iint_{bot} -J_C^p dx dy} \quad (7)$$

where S is the complete surface that surrounds the volume "Globe", and $\vec{n}$ is the outward normal unit vector of the surface S. The lower boundary "bot" of the global column is the surface of the Earth, and the upper boundary θ_T is a complete isentropic surface. According to Stokes' theorem, the integration on a surface of the normal component of relative vorticity equals the closed-loop circulation along the boundary surrounding the surface. Since there is no boundary for the upper surface θ_T, the first term on the right-hand side of Equation (7) vanishes, and the total amount of W in the entire bounded atmosphere becomes:

$$\underbrace{\iiint_{\text{Globe}} W dv} = \underbrace{\iint_{bot} -J_C^p dx dy} = \oiint [-(f + \zeta_s)\theta_s] ds \quad (8)$$

where the subscript "s" indicates the Earth's surface, and $[(f + \zeta_s)\theta_s]$ represents PVC at the surface. Taking time difference on Equation (8) leads to:

$$\underbrace{\iiint_{\text{Globe}} \frac{\partial}{\partial t} W dv} = \oiint \frac{\partial}{\partial t} [-(f + \zeta_s)\theta_s] ds \quad (9)$$

Equation (9) indicates that increase in surface $[-(f + \zeta_s)\theta_s]$ will lead to the increase in the PV substance (W) of the atmosphere. Therefore, a new variable:

$$SPV = [-(f + \zeta_s)\theta_s] \quad (10)$$

can be used as a factor to represent the PV forcing at the Earth's surface on the PV substance of the atmosphere.

3. Distributions of SPV and Index of the PV Forcing of the Tibetan Plateau

3.1. Global Distributions of SPV and Its Zonal Deviation

Figure 1 shows the spatial distributions of the climatic mean and the zonal deviation of SPV $[-(f + \zeta_s)\theta_s]$ in July, respectively. The climatic mean distribution (Figure 1a) is mainly determined by the distribution of the Coriolis parameter f presenting a zonal orientation feature and gradually decreasing from the south pole to the north pole. The zonal deviation distribution (Figure 1b) is characterized by a weak anomaly over the ocean and a strong anomaly over large terrain and plateaus, such as Greenland and the Rocky Mountains in North America, the Andes Mountains in South America, the Alps in Europe, and the Mongolia Plateau, Iranian Plateau, and Tibetan Plateau in Asia. Such a distribution of SPV is related to the fact that elevated mountains penetrate more isentropic surfaces in the lower troposphere and produce additional PV sources for the atmosphere [12]. The most remarkable negative area is on the Tibetan Plateau, indicating that the summertime negative SPV forcing is over land, particularly over the Tibetan Plateau.
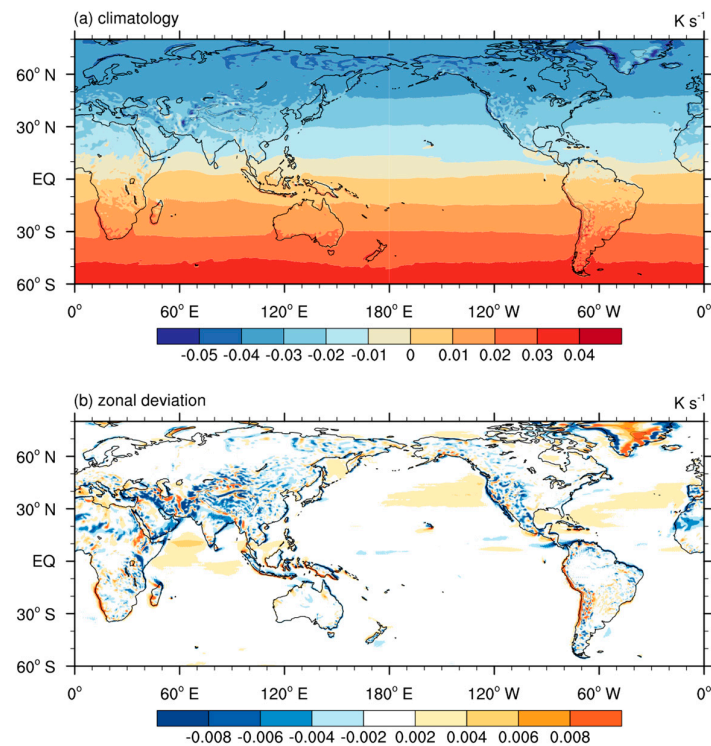
Figure 1. (**a**) Climatological July mean distribution of surface potential vorticity circulation (SPV, $[-(f + \zeta_s)\theta_s]$) and (**b**) its zonal deviation. Unit: K s^{-1}.

3.2. Index of the PV Forcing over the Tibetan Plateau

Figure 2 shows the first two empirical orthogonal function (EOF) modes of SPV on the Tibetan Plateau area higher than 3 km in July. The explanatory variance of the first EOF mode (EOF1) is 22.6%, showing a triple anomaly pattern of SPV with three anomalous centers over the northern, central, and southern Tibetan Plateau. The explanatory variance of EOF2 is 13.2%, which approximately presents a north-south reversed distribution across the plateau midline, implying a cyclonic circulation anomaly on the north and an anticyclonic circulation anomaly on the south, or vice versa. This mode mainly reflects the seesaw effect of SPV between the northern and southern Tibetan Plateau. To evaluate the relationships between these modes and the EASM, the East Asian monsoon intensity index is defined with reference to Wang et al. [2]: taking MV-EOF analysis on the three-dimensional circulation and precipitation in the East Asia region (0–50° N, 100–140° E), then define the principal component (PC) of the main mode as the intensity index of the East Asian monsoon (iEAM) in July. As both PC1 and PC2 of the SPV exhibit interannual variations, interannual relationships will be investigated in the following study.

The correlation coefficient between PC1 of the SPV and iEAM in July is only 0.05, beyond the 90% confidence level. As a result, PC1 and iEAM are approximately independent, whereas the correlation coefficient between PC2 of the SPV and iEAM is 0.54, exceeding the 99% confidence level based on Student's *t*-test. The high correlation between PC2 and iEAM indicates that the interannual variability of EASM is closely linked to the dipole mode of SPV over the Tibetan Plateau. Therefore, PC2 of the SPV over the Tibetan Plateau can be used to investigate the impacts of the PV forcing of the Tibetan Plateau on the EASM. According to Equation (9), the change in $[-(f + \zeta_s)\theta_s]$ will lead to the change of the PV substance W in the atmosphere. PC2 of SPV over the Tibetan Plateau is thus defined as the intrinsic PV forcing index of the plateau for the following study, which is abbreviated as "iPV":

$$iPV = PC2 \text{ of } [-(f + \zeta_s)\theta_s] \text{ over the Tibetan Plateau } (> 3 \text{ km}) \quad (11)$$

A positive iPV then corresponds to a positive (negative) PVC over the northern (southern) Tibetan Plateau, with surface westerly flows passing through the central plateau and affecting downstream circulations.
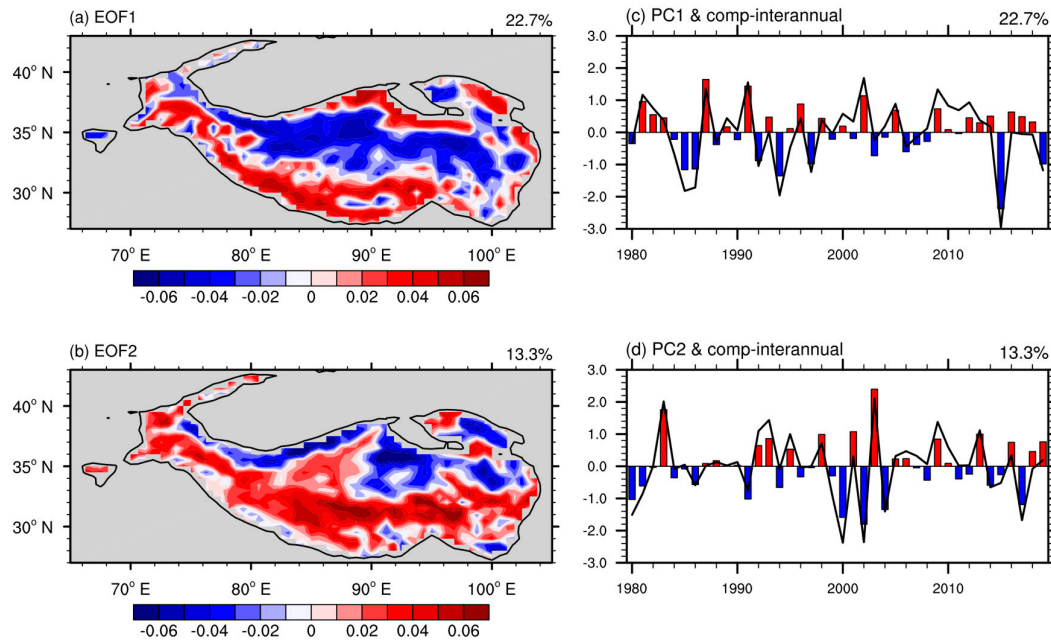

Figure 2. Spatial patterns of the first (**a**) and second (**b**) EOF modes of SPV on the Tibetan Plateau area higher than 3 km in July. (**c**,**d**) are the corresponding principal components, respectively, to (**a**,**b**) (black curve). The histogram in (**c**,**d**) represents the interannual variation after detrending during 1980–2019 and 2–9 years of bandpass filtering.

4. PV Forcing over the Tibetan Plateau on the EASM

The left column of Figure 3 shows the anomalies of the 200 hPa circulation and geopotential height (Figure 3a) and the 850 hPa circulation and precipitation (Figure 3b) regressed onto the iEAM index, representing the characteristic anomalous precipitation and circulation in the upper and lower troposphere in July for the strong EASM years. Its main characteristics are the presenting of a ray of circulation anomalies with anticyclone and cyclone centers located, respectively, over Mid Asia, northern Tibetan Plateau, the Jianghuai Basin, and Japan in the upper troposphere. The anticyclonic circulation anomaly centered over the Jianghuai Basin indicates the eastward shifting of the South Asian High at 200 hPa. In climatology, PV generally increases with latitude. The anomalous northerly flow associated with the anticyclonic circulation anomaly over East Asia thus favors the transport of positive PV anomaly to the Jianghuai region.

In the lower troposphere, the Jianghuai area is influenced by the enhanced Western Pacific subtropical high. The associated southwesterly anomaly transports much more water vapor and contributes to the positive precipitation anomaly over the Jianghuai region. In addition, the associated southwesterly anomaly transports negative PV anomaly to the Jianghuai area. Then the circulation background of PV advection increases with height forms, which is conducive to the development of air ascent [26–28], whereas the precipitation over the northern part of the South China Sea and near the Philippine Sea shows significant negative anomalies. The right column of Figure 3 is for the same variables but regressed onto the iPV index. The spatial anomalous patterns are very similar to their counterparts in the left column, particularly in their prominent circulation anomalies in the upper troposphere. This implies that there is an inextricable relationship between the in situ PV forcing over the Tibetan Plateau and the intensity of the EASM.
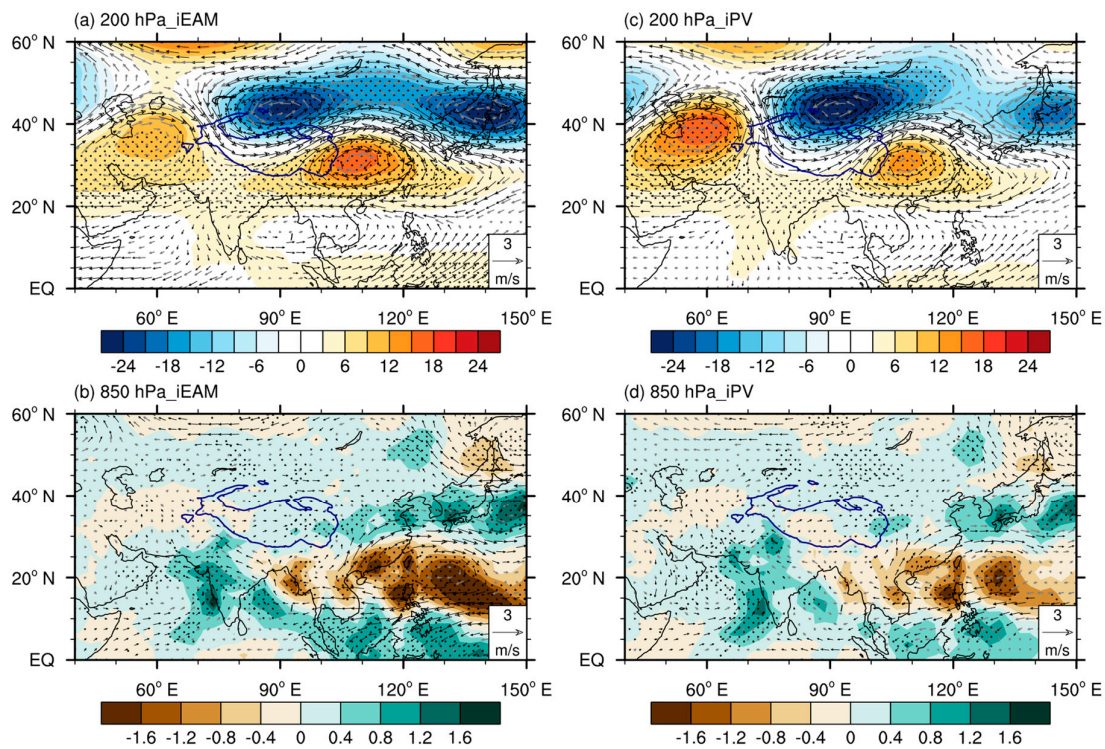
Figure 3. The 200 hPa wind (vector, unit: m s^{-1}) and geopotential height (shading, unit: gpm) anomaly (**a**,**c**) and the 850 hPa wind (vector, unit: m s^{-1}) and precipitation (shading, unit: mm day^{-1}) anomaly (**b**,**d**) regressed onto the iEAM index (**a**,**b**) and onto the iPV index (**c**,**d**).

To explore this relationship, we first investigate how the PV in the atmosphere over the plateau and the zonal PV flux downstream vary associated with the SPV over the plateau by regressing these fields onto the iPV index. Because the sign of EOF2 of SPV over the plateau is inverted on the northern and southern parts of the plateau (Figure 2b), the analysis is performed in two zonal-vertical cross sections located along 34–36° N in the north and 30–32° N in the south, respectively. As shown in Figure 4a,b, corresponding to a positive iPV, positive PV develops over the whole plateau in the north (Figure 4a) and its western part in the south (Figure 4b), presenting an upward and northward intensification of PV. Meanwhile, westerly flow predominates over the whole plateau, which will result in positive zonal PV advection in the upper troposphere and form a structure of PV advection increasing with height over the EASM region (Figure 4c,d). According to Hoskins et al. [26,27] and Wu et al. [28], air ascent will develop where PV advection increases with increasing height. Consequently, upward motion and precipitation develop over the EASM region.

Figure 5 presents the regression onto the iPV index of the vertically integrated (from 1000 to 300 hPa) water vapor flux and its divergence. The water vapor in the troposphere in the whole East Asia region is mainly transported through the anomalous southwesterly and westerly flow along the abnormal subtropical anticyclone over the northwestern Pacific. Significant water vapor divergence anomaly occurs within the anomalous subtropical anticyclone, whereas the anomalous southwesterly and westerly winds on the northwestern side of the anomalous subtropical anticyclone bring much more water vapor to the vicinity of the Jianghuai Basin, forming a large-scale water vapor convergence anomaly. As mentioned above, this anomalous pattern indicates the stronger EASM years with the strengthened western Pacific subtropical high which provides abundant water vapor conditions for the positive precipitation anomaly downstream of the Tibetan Plateau.
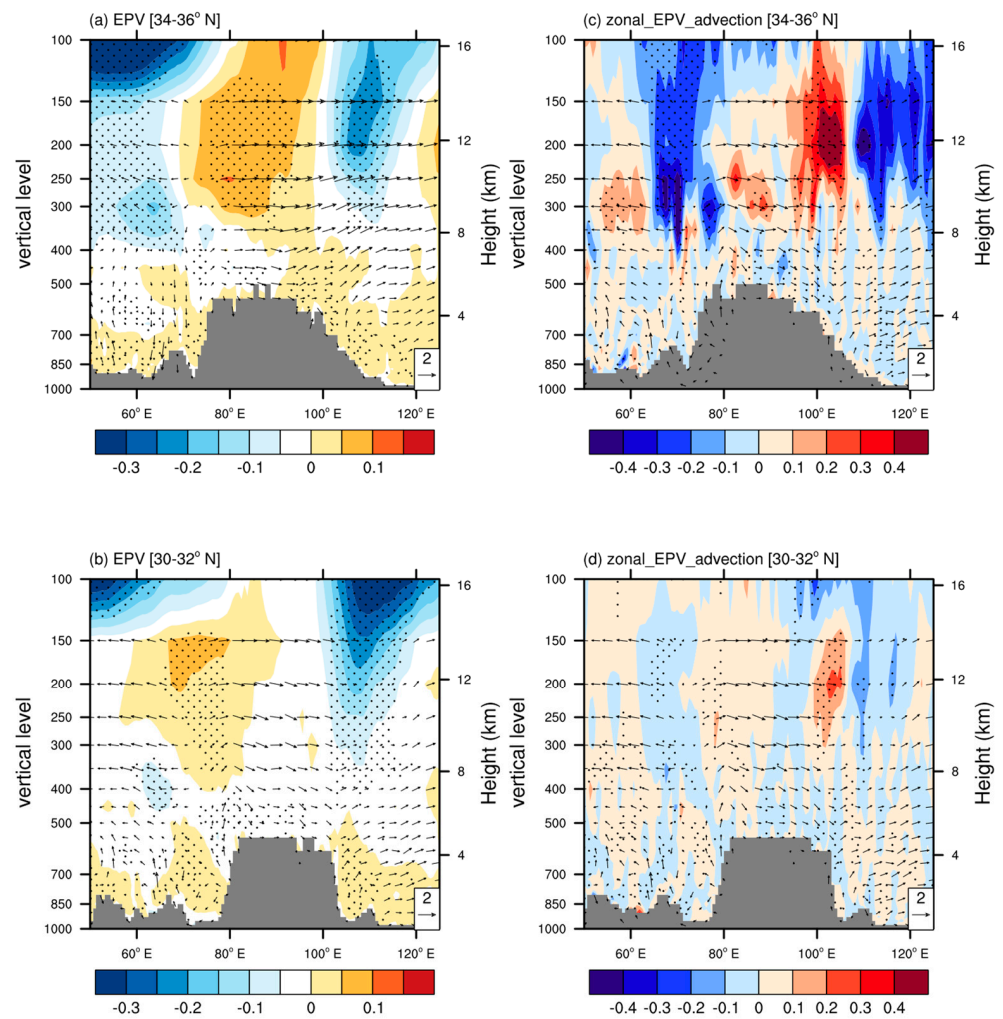
Figure 4. Zonal cross sections averaged over 34–36° N (**a**,**c**) and 30–32° N (**b**,**d**) of zonal circulation (vector, unit: m s^{-1}), and PV ((**a**,**b**); shading, unit: PVU, 1PVU = 10^{-6} K m^2 s^{-1} kg^{-1}) and zonal PV advection ((**c**,**d**); shading, unit: 10^{-5} PVU s^{-1}) regressed onto the iPV index.

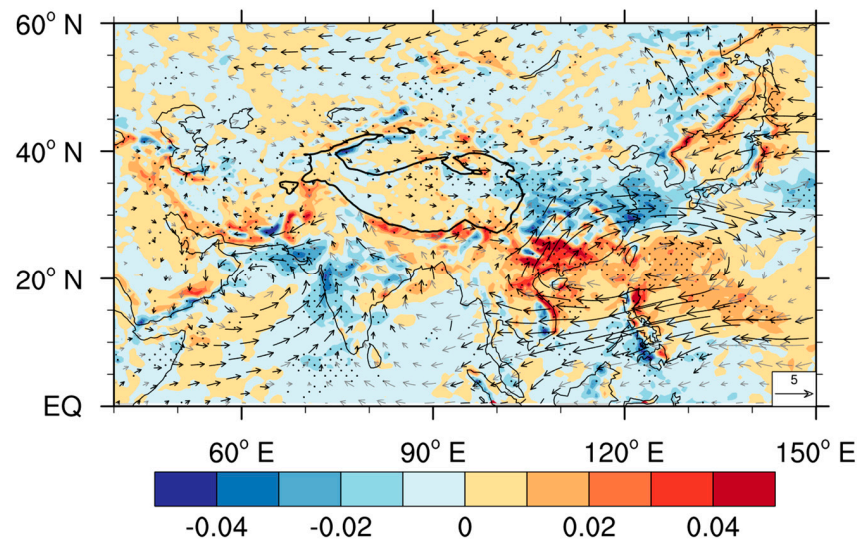**Figure 5.** The vertically integrated (from 1000 to 300 hPa) water vapor flux (vector, kg m^{-1} s^{-1}) and its divergence (shading, unit: 10^{-4} kg m^{-2} s^{-1}) regressed onto the iPV index.

The above analysis demonstrates that when the surface PVC over the Tibetan Plateau is in its positive phase of EOF2 with positive SPV on its south and negative SPV on its north (Figure 2b), prominent positive PV anomaly develops in the troposphere above the plateau platform accompanied with abnormally intensified westerly flows, forming a structure of zonal PV advection increasing with height in the troposphere of the downstream area, which is conducive to the generation of upward movement over the Jianghuai region. The upper troposphere over East Asia is controlled by the eastward-shifted South Asian High. The southwesterly wind anomaly on the northwest side of the Western Pacific subtropical high in the lower atmosphere transports abundant water vapor to the north, forming a convergence above the Jianghuai region. This not only enhances the typical anomaly of the three-dimensional circulation of the East Asian monsoon in July, but also further strengthens the formation of the Meiyu front, the main component of the EASM in July.

5. Relationship with the Overland Silk Road Pattern

Figures 3c and 4a demonstrate that the in situ positive PV forcing over the Tibetan Plateau corresponds well with the positive PV anomaly in the atmosphere over the plateau. To identify the link of this positive PV anomaly with the upper layer general circulation, the 200 hPa meridional wind distribution regressed onto the iPV index is shown in Figure 6. Significant southerly and northerly anomalies are concentrated in the mid-latitudes of Eurasia from the western Eurasian continent to East Asia. The structure of the meridional wind anomaly is similar to the SRP which also appears as alternate southerly and northerly anomalies along the mid-latitude Asian westerly jet from western Europe to East Asia [14,16]. The correlation coefficient between the iPV and the index of SRP (SRPI) is as high as 0.59, exceeding the significance level of 0.01.
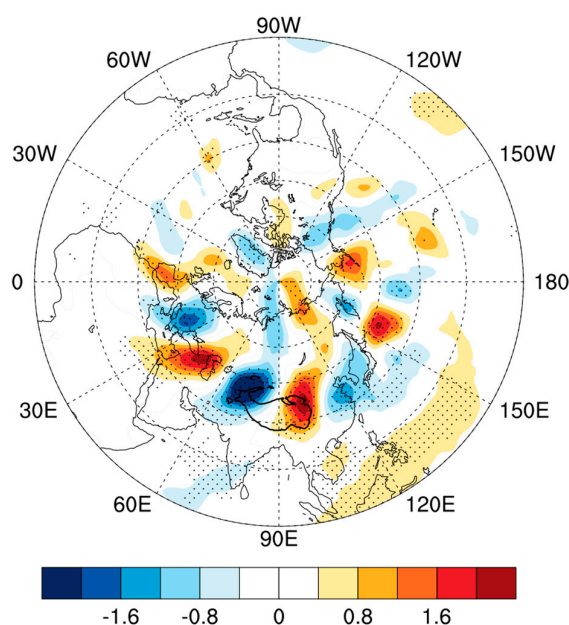

Figure 6. The distribution of the meridional wind anomaly at 200 hPa (shading, unit: m s^{-1}) regressed onto the iPV index. Areas exceeding the 0.05 significance level are highlighted by black dots.

Previous studies have shown that, through the associated anomalous northerly wind over East Asia, the summertime SRP has varying degrees of influence on the circulation and the precipitation in the East Asian areas [4,15,18,19,29]. In order to better understand the relationship between plateau PV forcing and the onland SRP in the influence of the interannual intensity of the EASM, we conduct two sets of partial correlation analysis: one by removing the linear influence of SRPI from that of iPV and the other by removing the linear influence of iPV from that of SRPI, and the results are presented in Figures 7 and 8, respectively.
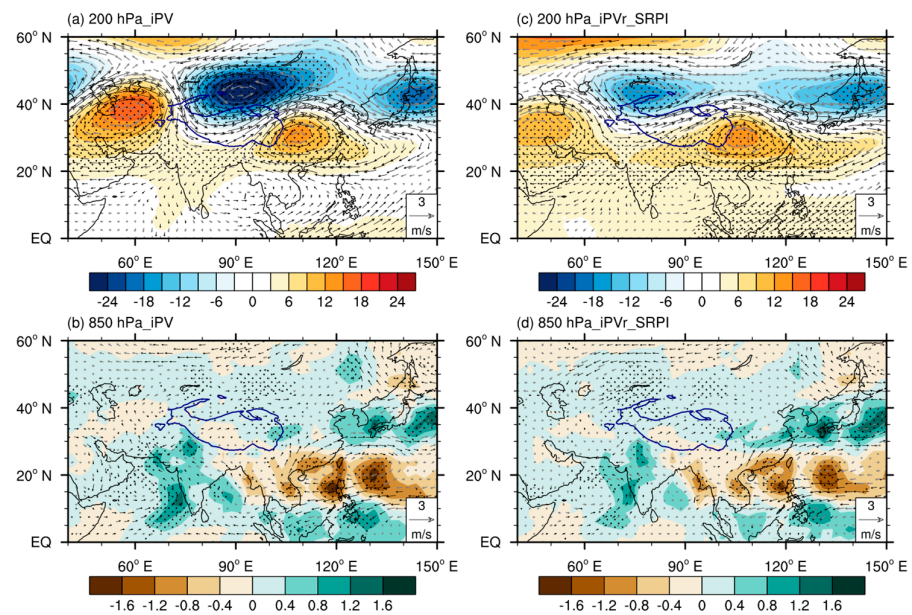
Figure 7. The distributions of circulation (vector, unit: m s^{-1}) and geopotential height (shading, unit: gpm) at 200 hPa (**a,c**) and the 850 hPa circulation (vector, unit: m s^{-1}) and precipitation (shading, unit: m day^{-1}) (**b,d**) regressed onto the iPV index (**a,b**) and regressed onto the iPVr index (**c,d**). iPVr represents the remaining time series after removing the linear correlation with SRPI from the iPV index. Dotted regions indicate the geopotential height and precipitation exceeding the 95% confidence level.

It can be seen from Figure 7 that when the linear influence of the SRP is removed, the distributions of circulation and precipitation anomalies in the lower tropospheric layer change little (Figure 7d) compared with the original distributions (Figure 7b). The main changes in the upper troposphere circulation are the weakening and westward shifting of the anomalous cyclone to the north of the Tibetan Plateau and its upstream anticyclonic anomaly (Figure 7c), while the position and intensity of the anomalous anticyclone over East Asia (Figure 7a) is almost unchanged (Figure 7c). The associated anomalous northerly wind still prevails over East Asia. As mentioned in Section 4 and previous studies [4,15], the northerly wind anomaly is a key factor that induces the precipitation anomaly over the Jianghuai region. Consequently, the results shown in Figure 7 indicate that no matter whether there is the influence of the SRP or not, PV forcing over the Tibetan Plateau can directly influence the intensity of EASM. The correlation coefficient between iPVr and iEAM is 0.49, which is only 0.05 lower than that between iPV and iEAM, but still reaches a significance level of 0.01. On the contrary, when the influence of plateau PV forcing is removed from the Silk Road tele-correlation, the regressed upper tropospheric circulation undergoes remarkable changes (Figure 8c versus Figure 8a). The strong cyclone anomaly to the north of the plateau (Figure 8a) becomes significantly weak and shifts southward (Figure 8c). The anomalous westerly wind prevailing over the entire plateau platform (Figure 8a) becomes much weaker and moves southward to the south of the plateau (Figure 8c). The downstream anticyclone anomaly originally located over the Jianghuai region moves northeastward and is located over Northeast China. The associated anomalous northerly wind moves northeastward correspondingly. The Jianghuai region is controlled by the easterly anomaly in the upper troposphere (Figure 8c). In the lower troposphere (Figure 8b,d), the subtropical anticyclone circulation over the northwestern Pacific is weakened, and no apparent precipitation anomalies occur in the Jianghuai area. The correlation coefficient between SRPIr and the overall East Asian monsoon intensity index iEAM drops to 0.01, which is almost independent. These results indicate that the SRP cannot influence the EASM directly in July. PV forcing over the Tibetan Plateau may play a role in "bridging" the connection between the EASM and the SRP.

The above results suggest that PV forcing over the Tibetan Plateau can directly influence the East Asian monsoon's variability. Such connection between the EASM and the plateau PV forcing in July is affected little by the SRP, whereas the plateau PV forcing plays a key role in "bridging" the SRP and the EASM precipitation. If the plateau PV forcing disappears, the upstream SRP may not have a significant effect on the East Asian summer monsoon.
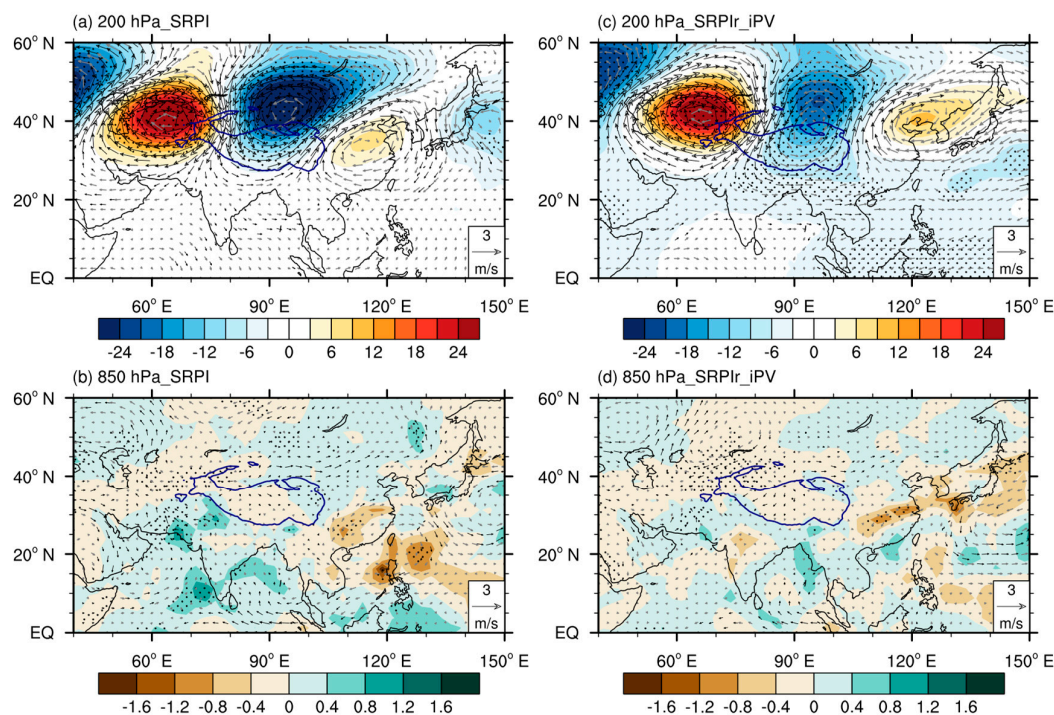

Figure 8. The distributions of circulation (vector, unit: m s^{-1}) and geopotential height (shading, unit: gpm) at 200 hPa (**a,c**) and the 850 hPa circulation (vector, unit: m s^{-1}) and precipitation (shading, unit: m day^{-1}) (**b,d**) regressed onto the SRPI index (**a,b**) and regressed onto the SRPIr index (**c,d**). SRPIr represents the remaining time series after removing the linear correlation with iPV from the SRPI index. Dotted regions indicate the geopotential height and precipitation exceeding the 95% confidence level.

6. Conclusions

By integrating the PV substance and its local change equation over the global atmospheric volume bounded by an enclosed isentropic surface as the upper boundary, it shows that the global gross PV substance equals the integral of the PV circulation (PVC) at the earth's surface of the whole globe. That means the gross source of PV substance of the global atmosphere is located at the Earth's surface. EOF analysis of the surface PV circulation (SPV) over the Tibetan Plateau higher than 3 km in July indicates that PC2 can be used as an index to characterize effects on the EASM of the intrinsic plateau PV forcing. By making partial correlation and regression analysis, this paper further studies the influence mechanism of the plateau PV forcing on the interannual variability of the EASM and its relationship with that of the onland SRP over Eurasia. The main conclusions can be summarized as follows:

(1)   When the second mode of SPV on the surface of the Tibetan Plateau platform is in the positive phase (Figure 2b), with positive SPV on its south and negative SPV on its north, a strong positive PV anomaly and strengthened westerly flow will develop in the troposphere over the plateau, forming a structure of zonal PV advection increasing with height in the troposphere over the downstream Jianghuai region, which is conducive to the generation of air ascent. The upper troposphere over East Asia is controlled by the strong positive anomaly of geopotential height due to

the eastward shifting of the South Asian High. The associated northerly anomaly favors the transport of positive PV anomaly to the Jianghuai region; whereas, in the lower troposphere, the anomalous southwesterly flow on the northwestern side of the enhanced western Pacific subtropical high transports not only abundant water vapor, but also negative PV anomaly to the Jianghuai region, forming a circulation background of PV advection increasing with height. This not only enhances the three-dimensional circulation anomaly of the East Asian monsoon in July, but also facilitates stronger precipitation along the Meiyu front;

(2) The link between East Asian monsoon variability and plateau PV forcing in July is influenced very little by the SRP. The latter mainly impacts the wave position and intensity in the upper troposphere to the west of the plateau, but has limited effect on the spatial distributions of circulation and precipitation downstream of the plateau. However, when the linear signal of plateau PV forcing is removed from the SRP sequence, the cyclone anomaly to the north of the plateau is significantly weakened and shifts southward. The westerly wind originally over the plateau becomes much weaker and shifts to the south of the plateau as well. At the same time, the anticyclone anomaly originally located over the Jianghuai region shifts to Northeast China. The Jianghuai region is controlled by the easterly anomaly in the upper troposphere, which weakens the circulation background of PV advection increasing with height. Consequently, the positive precipitation anomaly over the Jianghuai region becomes weak and the interannual variability of the SRP and the East Asian monsoon are no longer correlated. These results indicate that the SRP cannot influence the EASM directly in July. The plateau PV forcing plays a key role in "bridging" the influence of the SRP to the East Asian summer monsoon: the PV forcing over the Tibetan Plateau can modulate the influence of the SRP on the EASM by changing the position of the anticyclone anomaly in the upper troposphere downstream of the Tibetan Plateau which is critical for the development of air ascent and precipitation of the EASM. When the influence of plateau PV forcing is removed, this anticyclone anomaly is located over Northeast China, which has little impact on the EASM. However, when the influence of plateau PV forcing is considered, the anticyclone anomaly shifts to central China, contributing to a stronger EASM year. In other words, the influence of the SRP in the Eurasian region on the East Asian monsoon in July is inseparable from the involvement of the PV forcing over the Tibetan Plateau. In summary, it is the surface PV forcing of the Tibetan Plateau that directly and significantly affects the interannual variability of the EASM over the Jianghuai region.

Author Contributions: Y.L.: Conceptualization; validation; Funding acquisition; supervision; writing—review and editing. L.L.: Data curation; formal analysis; investigation; writing—original draft. G.W.: Conceptualization; Funding acquisition; writing—review and editing. T.M.: writing—review and editing. All authors have read and agreed to the published version of the manuscript.

Conflicts of Interest: The authors declare no conflict of interest.

References

1. Liu, F.; Ouyang, Y.; Wang, B.; Yang, J.; Ling, J.; Hsu, P.C. Seasonal evolution of the intraseasonal variability of China summer precipitation. *Clim. Dyn.* **2020**, *54*, 4641–4655. [CrossRef]
2. Wang, B.; Wu, Z.W.; Li, J.P.; Liu, J.; Chang, C.P.; Ding, Y.H.; Wu, G.X. How to measure the strength of the East Asian summer monsoon. *J. Clim.* **2008**, *21*, 4449–4463. [CrossRef]

3. Hong, X.W.; Lu, R.Y.; Li, S.L. Differences in the Silk Road Pattern and Its Relationship to the North Atlantic Oscillation between Early and Late Summers. *J. Clim.* **2018**, *31*, 9283–9292. [CrossRef]

4. Li, X.Y.; Lu, R.Y. Subseasonal change in the seesaw Pattern of Precipitation between the Yangtze River Basin and the Tropical Western North Pacific during Summer. *Adv. Atmos. Sci.* **2018**, *35*, 1231–1242. [CrossRef]

5. Wu, G.X.; Liu, Y.M.; Wang, T.M.; Wan, R.J.; Liu, X.; Li, W.P.; Wang, Z.Z.; Zhang, Q.; Duan, A.M.; Liang, X.Y. The influence of Mechanical and thermal forcing by the Tibetan Plateau on Asian climate. *J. Hydrometeorol.* **2007**, *8*, 770–789. [CrossRef]

6. Yeh, T.C. The circulation of the high troposphere over China in the winter of 1945–1946. *Tellus* **1950**, *2*, 173–183. [CrossRef]

7. Okajima, H.; Xie, S.P. Orographic effects on the northwestern Pacific monsoon: Role of air-sea interaction. *Geophys. Res. Lett.* **2007**, *34*, L21708. [CrossRef]

8. Yanai, M.; Li, C.; Song, Z. Seasonal heating of the Tibetan Plateau and its effects of the evolution of the Asian summer monsoon. *J. Meteor. Soc. Jpn.* **1992**, *70*, 319–351. [CrossRef]

9. Kitoh, A. Effects of large-scale mountains on surface climate—A coupled ocean atmosphere general circulation model study. *J. Meteorol. Soc. Jpn.* **2002**, *80*, 1165–1181. [CrossRef]

10. Duan, A.M.; Wu, G.X. Role of the Tibetan Plateau thermal forcing in the summer climate patterns over Subtropical Asia. *Clim. Dyn.* **2005**, *24*, 793–807. [CrossRef]

11. Sheng, C.; He, B.; Wu, G.X.; Liu, Y.M.; Zhang, S.Y. Interannual influences of the surface potential vorticity forcing over the Tibetan Plateau on East Asian summer rainfall. *Adv. Atmos. Sci.* **2022**, *39*, 1050–1061. [CrossRef]

12. Sheng, C.; Wu, G.X.; Tang, Y.Q.; He, B.; Xie, Y.K.; Ma, T.T.; Ma, T.; Li, J.X.; Bao, Q.; Liu, Y.M. Characteristics of the potential vorticity and its budget in the surface layer over the Tibetan Plateau. *Int. J. Climatol.* **2021**, *41*, 439–455. [CrossRef]

13. He, B.; Sheng, C.; Wu, G.X.; Liu, Y.M.; Tang, Y.Q. Quantification of seasonal and interannual variations of the Tibetan Plateau surface thermodynamic forcing based on the potential vorticity. *Geophys. Res. Lett.* **2022**, *49*, e2021GL097222. [CrossRef]

14. Lu, R.Y.; Oh, J.H.; Kim, B.J. A teleconnection pattern in upper-level meridional wind over the North African and Eurasian continent in summer. *Tellus* **2002**, *54*, 44–55. [CrossRef]

15. Ding, Y.H.; Wang, B. Circumglobal Teleconnection in the Northern Hemisphere Summer. *J. Clim.* **2005**, *18*, 3483–3505. [CrossRef]

16. Enomoto, T. Interannual Variability of the Bonin High Associated with the Propagation of Rossby Waves along the Asian Jet. *J. Meteorol. Soc. Jpn.* **2003**, *82*, 1019–1034. [CrossRef]

17. Hong, X.W.; Xue, S.H.; Lu, R.Y.; Liu, Y.Y. Comparison between the interannual and decadal components of the Silk Road pattern. *Atmos. Ocean. Sci. Lett.* **2018**, *11*, 270–274. [CrossRef]

18. Huang, R.H.; Chen, J.L.; Wang, L.; Lin, Z.D. Characteristics, processes, and causes of the spatio-temporal variabilities of the East Asian monsoon system. *Adv. Atmos. Sci.* **2012**, *29*, 910–942. [CrossRef]

19. Lin, S.M.; Hsu, H.H. Asymmetry of the Tripole Rainfall Pattern during the East Asian Summer. *J. Clim.* **2007**, *20*, 4443–4458.

20. Gelaro, R.; McCarty, W.; Suarez, M.J.; Todling, R.; Molod, A.; Takacs, L.; Randles, C.A.; Darmenov, A.; Bosilovich, M.G.; Reichle, R.; et al. The Modern-Era Retrospective Analysis for Research and Applications, Version 2 (MERRA-2). *J. Clim.* **2017**, *30*, 5419–5454. [CrossRef]

21. Adler, R.F.; Huffman, G.J.; Chang, A.; Ferraro, R.; Xie, S.P.; Janowiak, J.; Rudolf, B.; Schneider, U.; Curtis, S.; Bolvin, D.; et al. The Version-2 Global Precipitation Climatology Project (GPCP) Monthly Precipitation Analysis (1979–Present). *J. Hydrometeorol.* **2003**, *4*, 1147–1167. [CrossRef]

22. Huang, J.Y. *Statistical Analysis Method of Meteorological Data*, 4th ed.; China Meteorological Press: Beijing, China, 2016; p. 25, ISBN 978-7-5029-6346-0. (In Chinese)

23. Haynes, P.H.; McIntyre, M.E. On the evolution of vorticity and potential vorticity in the presence of diabatic heating and frictional or other forces. *J. Atmos. Sci.* **1987**, *44*, 828–841. [CrossRef]

24. Haynes, P.H.; McIntyre, M.E. On the conservation and impermeability theorems for potential vorticity. *J. Atmos. Sci.* **1990**, *47*, 2021–2031. [CrossRef]

25. Sheng, C.; Wu, G.X.; He, B.; Liu, Y.M.; Ma, T.T. Linkage between cross-equatorial potential vorticity flux and surface air temperature over the mid-high latitudes of Eurasia during boreal spring. *Clim. Dyn.* **2022**, *59*, 3247–3263. [CrossRef]

26. Hoskins, B.J.; McIntyre, M.E.; Robertson, A.W. On the use and significance of isentropic potential vorticity maps. *Q. J. R. Meteorol. Soc.* **1985**, *111*, 877–946. [CrossRef]

27. Hoskins, B.J.; Pedder, M.; Jones, D.W. The omega equation and potential vorticity. *Q. J. R. Meteorol. Soc.* **2003**, *129*, 3277–3303. [CrossRef]

28. Wu, G.X.; Ma, T.T.; Liu, Y.M.; Jiang, Z.H. PV-Q Perspective of Cyclogenesis and Vertical Velocity Development Downstream of the Tibetan Plateau. *J. Geophys. Res. Atmos.* **2020**, *125*, e2019JD030912. [CrossRef]

29. Lu, R.Y.; Li, X.Y. Extratropical Factors Affecting the Variability in Summer Precipitation over the Yangtze River Basin, China. *J. Clim.* **2019**, *30*, 8357–8374.